

Variations of Casimir energy from a superconducting transition

Giuseppe Bimonte, Enrico Calloni, Giampiero Esposito and Luigi Rosa
*Dipartimento di Scienze Fisiche, Università di Napoli Federico II,
Via Cintia I-80126 Napoli, Italy; INFN, Sezione di Napoli, Napoli, ITALY*
(Dated: November 5, 2018)

We consider a five-layer Casimir cavity, including a thin superconducting film. We show that when the cavity is cooled below the critical temperature for the onset of superconductivity, the sharp variation (in the microwave region) of the reflection coefficient of the film produces a variation in the value of the Casimir energy. Even though the relative variation in the Casimir energy is very small, its magnitude can be comparable to the condensation energy of the superconducting film, and thus causes a significant increase in the value of the critical magnetic field, required to destroy the superconductivity of the film. The proposed scheme might also help clarifying the current controversy about the magnitude of the contribution to Casimir free energy from the TE zero mode, as we find that alternative treatments of this mode strongly affect the shift of critical field.

PACS numbers: 12.20.Ds, 42.50.Lc

Keywords: Casimir effect, superconductors, film, critical field

I. INTRODUCTION

In recent years, new and exciting advances in experimental techniques [1] prompted a great revival of interest in the Casimir effect, over fifty years after its theoretical discovery [2] (for a recent review on both theoretical and experimental aspects of the Casimir effect, see Refs. [3]-[6]). As is well known, this phenomenon is a manifestation of the zero-point fluctuations of the electromagnetic field: it is a purely quantum effect and it constitutes one of the rare instances of quantum phenomena on a macroscopic scale.

In his famous paper, Casimir evaluated the force between two parallel, electrically neutral, perfectly reflecting plane mirrors, placed a distance L apart, and found it to be attractive and of a magnitude equal to:

$$F_C = \frac{\hbar c \pi^2 A}{240 L^4}. \quad (1)$$

Here, A is the area of the mirrors, which is supposed to be much larger than L^2 , so that edge effects become negligible. The associated energy E_C

$$E_C = -\frac{\hbar c \pi^2 A}{720 L^3}. \quad (2)$$

can be interpreted as representing the shift in the zero-point energy of the electromagnetic field, between the mirrors, when they are adiabatically moved towards each other starting from an infinite distance. The Casimir force is indeed the dominant interaction between neutral bodies at the micrometer or submicrometer scales, and by modern experimental techniques it has now been measured with an accuracy of a few percent (see Refs. [1] and Refs. therein).

The issue of the energy of vacuum fluctuations, a manifestation of which is provided by the Casimir effect, is of the utmost importance in other areas of Physics, most notably in Cosmology, where it is known to raise a number of problems, when its gravitational effects are

considered [7]. For this reason, it is clearly very important to devise laboratory tests to study the physical consequences of vacuum fluctuations, as a way to check our theoretical understanding of this intriguing quantum phenomenon.

All experiments on the Casimir effect performed so far measured the Casimir force, in a number of different geometric configurations. In a recent Letter [8] we have found that by realizing a rigid cavity, including a superconducting film, it should be possible to measure directly the variation of Casimir energy accompanying the transition to the normal state of the superconducting film, in an external magnetic field.

Apart from the fundamental interest of a direct measurement of a (variation of) Casimir energy, rather than a force, our scheme has the further advantage that, being based on rigid cavities, it should make it easier to study the dependence of the Casimir effect on the geometry of the cavity. Indeed, since this effect arises from long-range correlations between the dipole moments of the atoms forming the walls of the cavity, that are induced by coupling with the fluctuating electromagnetic field, the Casimir energy depends in general on the geometric features of the cavity. For example, we see from Eq. (2) that, in the simple case of two parallel slabs, the Casimir energy E_C is negative and is not proportional to the volume of the cavity, as would be the case for an extensive quantity, but actually depends separately on the area and distance of the slabs. Indeed, the dependence of E_C on the geometry of the cavity can reach the point where it turns from negative to positive, leading to repulsive forces on the walls. For example (see Ref. [3]), in the case of a cavity with the shape of a parallelepiped, the sign of E_C depends on the ratios among the sides, while in the case of a sphere it has long been thought to be positive. It is difficult to give a simple intuitive explanation of these shape effects, as they hinge on a delicate process of renormalization, in which the finite final value of the Casimir energy is typically expressed as a differ-

ence among infinite positive quantities. In fact, there exists a debate, in the current literature, whether some of these results are true or false, being artifacts resulting from an oversimplification in the treatment of the walls [10]. Under such circumstances, we think it would be desirable to have the possibility of an experimental check of these statements, for the maximum possible variety of configurations.

Another reason of interest in our superconducting cavities, not discussed in [8], is that their study will help clarifying one of the most debated issues in the current literature on the Casimir effect, i.e. the question of the contribution from the TE zero mode to thermal corrections in real metals, i.e. characterized by a finite conductivity. At the present time, there is no general agreement between the experts on how to deal with this problem, and we address the reader to Refs. [11] for a survey of the extended literature on this topic. A superconducting cavity is a very good tool to explore this problem, because the variation of Casimir energy across the transition precisely arises from the fact that the film has a finite conductivity, that changes when it becomes superconducting. Indeed, the computations presented in Sec. IV show that the critical field required to destroy the superconductivity of our cavity is very sensitive to the contribution of the TE zero mode, at the level that the alternative treatments proposed in the literature may lead to predictions that can differ even by 100 percent.

The plan of the paper is as follows. In Sect. II we present the general scheme of superconducting Casimir cavities, in Sec. III we discuss the applicability of Lifshitz theory [12] to the computation of the variation of Casimir energy in the superconducting transition. In Sec. IV we present the results of our numerical computations, including in Subsec. C a study of the contribution from the TE zero mode and finally, in Sec. V, we draw some conclusions and outline possible future work. We have included two Appendices to review the basic facts on type I superconductors that are useful to understand the properties of our superconducting cavities.

II. THE SUPERCONDUCTING CAVITY

The Casimir cavity that we consider is the planar five-layer system depicted in Fig. 1: a thin superconducting film of thickness D is placed between two thick metallic slabs (made of a non-magnetic and non superconducting metal), that constitute the plates of the cavity. The gaps of width L separating the film from the plates are supposed to be filled with some insulating material.

We consider cooling the cavity at a temperature T below the critical temperature T_c for the onset of superconductivity in the thin film. A magnetic field parallel to the film is then turned on, and its intensity is gradually increased, until it reaches the critical value $H_{c\parallel}$, for which superconductivity of the film is destroyed. The question we ask is whether the Casimir energy stored in the cavity

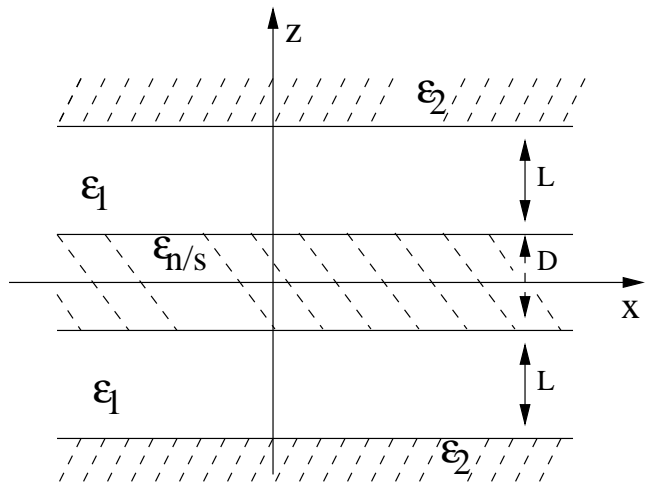


FIG. 1: Scheme of the superconducting five-layer cavity.

affects in an appreciable way the value of $H_{c\parallel}$. To address this question (see Appendix I for a short review of the magnetic properties of type I superconductors), we start from Eq. (A10) that connects $H_{c\parallel}$ to the (density of) condensation energy $e(T)$ of the film. Upon multiplying both sides of Eq. (A10) by the volume V occupied by the film, we obtain:

$$\frac{V}{8\pi} \left(\frac{H_{c\parallel}(T)}{\rho} \right)^2 = \mathcal{E}_{\text{cond}}(T), \quad (3)$$

where $\mathcal{E}_{\text{cond}}(T) = V e(T)$ is the condensation energy of the film. When the film is included in a cavity, the r.h.s. of the above Equation should be augmented by an extra term, i.e. the $\Delta F_E^{(C)}(T)$ representing the *difference*

$$\Delta F_E^{(C)}(T) := F_n^{(C)}(T) - F_s^{(C)}(T) \quad (4)$$

among the Casimir free energies of the cavity, in the superconducting (s) and in the normal (n) states of the film (in zero magnetic field). While we postpone to the next Section the computation of $\Delta F_E^{(C)}(T)$, we observe here that the presence of such a term should be expected on physical ground, because the transition to superconductivity causes a sharp variation in the reflective power of a film in the microwave region of the spectrum [13], and this obviously produces a change in the Casimir energy, which depends on the reflection coefficients of the plates. Thus, for the cavity case, Eq. (3) should be replaced by

$$\frac{V}{8\pi} \left(\frac{H_{c\parallel}^{\text{cav}}(T)}{\rho} \right)^2 = \mathcal{E}_{\text{cond}}(T) + \Delta F_E^{(C)}(T). \quad (5)$$

In writing this equation, the assumption has been made that the value of the coefficient ρ does not change when a film is placed in a cavity. This approximation amounts to saying that all quantities referring to the film, like the penetration depth, condensation energy etc. are not affected by virtual photons in the surrounding cavity. This

is a very good approximation, since the leading effect of radiative corrections is a small renormalization of the electron mass [14] of order $\varepsilon := \alpha \times \hbar\omega_c/(mc^2)$ (up to logarithmic corrections), where α is the fine structure constant, $\omega_c = c/L$ is the typical angular frequency of virtual photons, and m is the electron mass. Even for L as small as 10 nm, $\varepsilon \approx 3 \times 10^{-7}$. The associated shift of critical field is of the same order of magnitude, and thus negligible with respect to that caused by $\Delta F_E^{(C)}$, which will turn out to be of some percent (see Sec. IV).

Equation (5) deserves further comments. Consider first the relative shift of parallel critical field:

$$\frac{\delta H_{c\parallel}}{H_{c\parallel}} := \frac{H_{c\parallel}^{\text{cav}} - H_{c\parallel}}{H_{c\parallel}}, \quad (6)$$

which, according to Eqs. (3) and (5), is equal to

$$\frac{\delta H_{c\parallel}}{H_{c\parallel}} = \sqrt{\frac{\Delta F_E^{(C)}}{\mathcal{E}_{\text{cond}}} + 1} - 1. \quad (7)$$

Now, the relative variation $\Delta F_E^{(C)}/F_n^{(C)}$ of Casimir energy should be expected a very small number, because the Casimir energy is mostly associated with photon energies of order $\hbar\omega_c$, i.e. $10 \div 20$ eV for $L \simeq 10$ nm, while the transition to superconductivity affects the reflective power only at photon energies of order $kT_c \approx 10^{-4}$ eV for $T_c \simeq 1$ K. However, and this is the key point, Eq. (7) shows that *the shift of critical field is determined by the variation of Casimir free energy $\Delta F_E^{(C)}$ as compared to the condensation energy $\mathcal{E}_{\text{cond}}$ of the film.* The latter is very small: for a thin film with, say, an area A of 1 cm² (the area A is not really important, because for $A \gg L^2$ both $\mathcal{E}_{\text{cond}}$ and $\Delta F_E^{(C)}$ are proportional to A) and a thickness of a few nm it is easily of order 10^{-8} erg. By contrast, we see from Eq. (2) that a typical Casimir energy for a cavity with an area of 1 cm² and a width $L = 10$ nm, has a magnitude of 0.43 erg, i.e. over seven orders of magnitude larger than the condensation energy of the film. This implies that even a relative variation of Casimir energy as small as one part in 10^8 would still correspond to more than 10% of the condensation energy of the film, and would induce a shift of critical field of over 5 %.

The huge increase in sensitivity that we predict by virtue of a second energy scale, the condensation energy, which is orders of magnitude smaller than the scale characteristic of the Casimir effect, is the marking difference between our scheme and previous attempts at a direct measurement of the relative variation of the Casimir force, caused by a change in the reflective power of the mirrors. For example, Ref. [15] reports on an experiment, based on the technology of hydrogen switchable mirrors. Despite the large modulation of reflectivity in the optical region of the spectrum, which is very relevant for typical submicron separations between the mirrors, no detectable variation in the Casimir force could be seen,

possibly due to lack of the necessary sensitivity in force measurements.

Another comment on Eq. (7) is in order. As we shall see in Sec. IV, and what is a distinctive feature of the Casimir effect, the variation of Casimir energy $\Delta F_E^{(C)}$ turns out to depend on L , while the condensation energy does not. This implies an L dependence of the shift of critical field, which, if seen, would be strong evidence for the Casimir origin of the effect. In this respect, we notice that having chosen for the outer plates a non superconducting material, we do not have to worry about possible L -dependent Josephson couplings among the film and the lateral plates, that could produce a similar effect.

III. CALCULATION OF THE VARIATION OF CASIMIR ENERGY IN THE SUPERCONDUCTING TRANSITION

In this Section, we show how to compute the difference among the Casimir free energies of the cavity, in the superconducting (s) and in the normal (n) states of the film (in zero magnetic field). In this computation we shall use the generalization to multilayer systems of the theory developed by Lifshitz [12] to compute the van der Waals and Casimir energy for a plane-parallel cavity formed by two thick dielectric walls separated by an empty gap.

Before we turn to this computation, it is however necessary to discuss first the applicability of the Lifshitz theory to a superconducting cavity. Another concern is to ascertain whether we can use that theory to reliably evaluate $\Delta F_E^{(C)}(T)$ for separations L and for film thicknesses D as small as a few nm, which are the values of interest for us. Now, the main assumption of Lifshitz theory is that, *in the relevant range of frequencies and wave vectors*, one can describe the propagation of electromagnetic waves inside the media forming the cavity, in terms of a complex permittivity, depending only on the frequency ω . It is important to stress that the theory includes also non-retarded effects, and hence it has as limiting cases both van der Waals forces (that become important at small distances, like those we consider) and Casimir forces. On this ground, it has been used recently to study van der Waals interactions among thin metal films (of thickness about 10 Å), till very small separations (a few Å) [16].

When spatial non-locality effects become important, so that the complex permittivity becomes a function also of the wave vector \mathbf{q} , the Lifshitz theory is no longer applicable [17](see also the discussion on p.126 in Ref. [3]). Now it is clear that non-local effects are important, in general, in superconductors, by virtue of the very small skin depth (of the order of the penetration depth λ , typically 500 Å or so) also in the frequency region characteristic of the normal skin effect in normal metals (for an interesting discussion of non-local effects in the computation of dispersion forces in superconductors, see Ref. [18]). Moreover, for small separations L , as well as for

small film thicknesses $D < 25 - 30$ nm and/or at cryogenic temperatures non-local effects become important also in the normal state [19], and indeed it has been advocated that space dispersion should be taken into account, for example, to evaluate the influence of thin metal coatings, that are used to protect the plates in most of the current experiments on the Casimir effect (see [3] and last of Refs.[19]). The influence of space dispersion on the Casimir effect at room temperature is studied also in the recent paper [20]). These considerations lead to the conclusion that, for a reliable evaluation of the *individual* Casimir free energies $F_n^{(C)}(T)$ and $F_s^{(C)}(T)$, it is necessary to consider space dispersion. However, and this is a key point, space dispersion is unimportant for the purpose of computing the *difference* $\Delta F_E^{(C)}(T)$ between the Casimir energies in the two states of the film, which is the only quantity of interest for us. The reason is that the optical properties of thin films (with a thickness D much smaller than the skin depth or correlation length ξ), in the normal and in the superconducting states, are indistinguishable for photon energies larger than a few times kT_c , as accurate measurements have shown [13]. This implies that, in the computation of $\Delta F_E^{(C)}$, the only relevant photon energies are those below a few times kT_c (corresponding to the far IR), which is where the optical properties of the film actually change when it becomes superconducting. In this wavelength region, the quoted experiment shows that the transmittivity data for thin superconducting films can be well interpreted in terms of a complex permittivity that depends only on the fre-

quency, and is independent of the film thickness.

Having established the applicability of the Lifshitz theory to our superconducting cavity, we recall that in the original treatment by Lifshitz, dealing with two thick dielectric slabs separated by an empty gap, the Casimir force was obtained by evaluating, at points in the gap region, the Maxwell stress tensor associated with the electromagnetic fields generated by the randomly fluctuating currents in the interior of the dielectric slabs. Although physically transparent, this approach has never been extended to multilayer systems, due to the complexity of the computations that are involved. The desired generalization can however be obtained by using an alternative approach, similar to the one used by Casimir himself in his study of an ideal metallic cavity, in which the Casimir energy is obtained as the zero-point energy of the electromagnetic field inside the cavity. This method was applied to dielectric cavities in Refs. [21], where it was shown that one recovers the Lifshitz result, and was later generalized to multilayer systems in Ref. [22].

We thus consider the five-layer system depicted in Fig. 1. The electric permittivities of the layers are denoted as follows: $\epsilon_{n/s}$ represents the permittivity of the film, in the n/s states respectively, while ϵ_1 is the permittivity of the insulating layers. Last, ϵ_2 is the permittivity of the outermost thick normal metallic plates.

We consider first the $T = 0$ case. Then, the Casimir free energy coincides with the Casimir energy $E^{(C)}$, and we can write the unrenormalized variation of Casimir energy $\Delta E_0^{(C)}(L, D)$ as

$$\Delta E_0^{(C)}(L, D) = A \frac{\hbar}{2} \int \frac{dk_1 dk_2}{(2\pi)^2} \left\{ \sum_p (\omega_{\mathbf{k}_\perp, p}^{(n, TM)} + \omega_{\mathbf{k}_\perp, p}^{(n, TE)}) - \sum_p (\omega_{\mathbf{k}_\perp, p}^{(s, TM)} + \omega_{\mathbf{k}_\perp, p}^{(s, TE)}) \right\}, \quad (8)$$

where $A \gg L^2$ is the area of the cavity, $\mathbf{k}_\perp = (k_1, k_2)$ denotes the two-dimensional wave vector in the xy plane, while $\omega_{\mathbf{k}_\perp, p}^{(n/s, TM)}$ ($\omega_{\mathbf{k}_\perp, p}^{(n/s, TE)}$) denote the proper frequencies of the TM (TE) modes, in the n/s states of the film, respectively.

Upon using the argument theorem, and by subtracting the contribution corresponding to infinite separation L (for details, we address the reader to Chap. 4 in Ref. [3]) [35], we can rewrite the renormalized sums in Eq. (8) as integrals over *complex* frequencies $i\zeta$:

$$\left(\sum_p \omega_{\mathbf{k}_\perp, p}^{(n, TM)} - \sum_p \omega_{\mathbf{k}_\perp, p}^{(s, TM)} \right)_{\text{ren}} = \frac{1}{2\pi} \int_{-\infty}^{\infty} d\zeta \left(\log \frac{\Delta_n^{(1)}(i\zeta)}{\tilde{\Delta}_n^{(1)}(i\zeta)} - \log \frac{\Delta_s^{(1)}(i\zeta)}{\tilde{\Delta}_s^{(1)}(i\zeta)} \right), \quad (9)$$

where $\Delta_{n/s}^{(1)}(i\zeta)$ is the expression in Eq. (4.7) of [3] (evaluated for $\epsilon_0 = \epsilon_{n/s}$) and $\tilde{\Delta}_{n/s\infty}^{(1)}(i\zeta)$ denotes the asymp-

totic value of $\Delta_{n/s}^{(1)}(i\zeta)$ in the limit $L \rightarrow \infty$ (corresponding to the limit $d \rightarrow \infty$ with the notation of [3]). A similar expression can be written for the TE modes, which

involves the quantity $\Delta_{n/s}^{(2)}(i\zeta)$ defined in Eq. (4.9) of [3]. Upon inserting Eq. (9), and the analogous expression for TE modes, into Eq. (8) one gets the following expres-

$$\Delta E^{(C)} = A \frac{\hbar}{2} \int \frac{d\mathbf{k}_\perp}{(2\pi)^2} \int_{-\infty}^{\infty} \frac{d\zeta}{2\pi} \left(\log \frac{Q_n^{TE}}{Q_s^{TE}} + \log \frac{Q_n^{TM}}{Q_s^{TM}} \right), \quad (10)$$

where we set

$$Q_I^{(TM/TE)}(\zeta) \equiv \frac{\Delta_I^{(1/2)}(i\zeta)}{\Delta_{I\infty}^{(1/2)}(i\zeta)}, \quad I = n, s. \quad (11)$$

Upon performing the change of variables $k_\perp^2 = (p^2 - 1)\zeta^2/c^2$ in the integral over k_\perp , the above expression for $\Delta E^{(C)}(L, D)$ turns into

$$\Delta E^{(C)} = \frac{\hbar A}{4\pi^2 c^2} \int_1^\infty p dp \int_0^\infty d\zeta \zeta^2 \left(\log \frac{Q_n^{TE}}{Q_s^{TE}} + \log \frac{Q_n^{TM}}{Q_s^{TM}} \right), \quad (12)$$

where the explicit expression of the coefficients $Q_I^{(TM/TE)}$ is

$$Q_I^{TE/TM}(\zeta, p) = \frac{(1 - \Delta_{1I}^{TE/TM} \Delta_{12}^{TE/TM} e^{-2\zeta K_1 L/c})^2 - (\Delta_{1I}^{TE/TM} - \Delta_{12}^{TE/TM} e^{-2\zeta K_1 L/c})^2 e^{-2\zeta K_I D/c}}{1 - (\Delta_{1I}^{TE/TM})^2 e^{-2\zeta K_I D/c}}, \quad (13)$$

$$\Delta_{jl}^{TE} = \frac{K_j - K_l}{K_j + K_l}, \quad \Delta_{jl}^{TM} = \frac{K_j \epsilon_l(i\zeta) - K_l \epsilon_j(i\zeta)}{K_j \epsilon_l(i\zeta) + K_l \epsilon_j(i\zeta)}, \quad K_j = \sqrt{\epsilon_j(i\zeta) - 1 + p^2}, \quad I = n, s; \quad j, l = 1, 2, n, s. \quad (14)$$

Formulae along similar lines, involving the reflection coefficients of the layers, have been obtained for example in Refs.[23].

The extension of the above formulae to the case of finite temperature is straightforward. As is well known this amounts to the replacement in Eq. (10) of the integration

$\int d\zeta/2\pi$ by the summation $kT/\hbar \sum_l$ over the Matsubara frequencies $\zeta_l = 2\pi l/\beta$, where $\beta = \hbar/(kT)$, which leads to the following expression for the variation $\Delta F_E^{(C)}(T)$ of Casimir free energy:

$$\Delta F_E^{(C)}(T) = A \frac{kT}{2} \sum_{l=-\infty}^{\infty} \int \frac{d\mathbf{k}_\perp}{(2\pi)^2} \left(\log \frac{Q_n^{TE}}{Q_s^{TE}} + \log \frac{Q_n^{TM}}{Q_s^{TM}} \right). \quad (15)$$

As we see, Eqs. (12-15) involve the electric permittivities $\epsilon(i\zeta)$ of the various layers at imaginary frequencies $i\zeta$. For these functions, we have made the following choices.

For the outermost metal plates, we use a Drude model

for the electric permittivity:

$$\epsilon_D(\omega) = 1 - \frac{\Omega^2}{\omega(\omega + i\gamma)}, \quad (16)$$

where Ω is the plasma frequency and $\gamma = 1/\tau$, with

τ the relaxation time. We denote by Ω_2 and τ_2 the values of these quantities for the outer plates. As is well known, the Drude model provides a very good approximation in the low-frequency range $\omega \approx 2kT_c/\hbar \simeq 10^{11} \div 10^{12}$ rad/sec which is involved in the computation of $\Delta F_E^{(C)}(T)$ and $\Delta E^{(C)}$. The relaxation time is temperature dependent and for an ideal metal it becomes infinite at $T = 0$. However, in real metals, the relaxation time stops increasing at sufficiently low temperatures (typically of the order of a few K), where it reaches a saturation value, which is determined by the impurities that are present in the metal. Since in a superconducting cavity the temperatures are very low, we can assume that τ_2 has reached its saturation value and therefore we can treat it as a constant. The continuation of Eq. (16) to the imaginary axis is of course straightforward and gives

$$\epsilon_D(i\zeta) = 1 + \frac{\Omega^2}{\zeta(\zeta + \gamma)}. \quad (17)$$

For the insulating layers, we take a constant permittivity, equal to the static value:

$$\epsilon_1(\omega) = \epsilon_1(0). \quad (18)$$

Again, this is a good approximation in the range of frequencies that we consider.

As for the film, in the normal state we use again the Drude expression Eq. (16), with appropriate values for the plasma frequency Ω_n and the relaxation time τ_n .

The permittivity $\epsilon_s(i\zeta)$ of the film in the superconducting state cannot be given in closed form and we have evaluated it as explained in Appendix B, starting from the Mattis–Bardeen formula for the conductivity $\sigma_s(\omega)$ of a superconductor in the local limit $q \rightarrow 0$ of BCS theory.

IV. NUMERICAL COMPUTATIONS

In this Section we present the results of our numerical computations. For the convenience of the reader, the material is divided into four separate Subsections. In the first Subsection we analyze the qualitative features to be expected from a numerical evaluation of Eqs. (10)–(15). In Subsec. B we present the computation of the variation $\Delta F_E^{(C)}$ of Casimir free energy in the superconducting transition. In Subsec. C we discuss the controversial issue of the contribution arising from the TE zero mode. Finally, in the last Subsection, we present our results for the shift of critical magnetic field.

A. Qualitative features of $\Delta F_E^{(C)}$

In this Subsection we discuss some qualitative features of Eqs. (10)–(15) that are useful as a check of the numerical computations. We recall first of all that, with our choices for the cavity geometry and for the permittivities

of the various layers, the value of $\Delta F_E^{(C)}$ depends on the following sets of parameters:

1. the thickness of the film D and the width of the insulating gaps L (see Fig. 1);
2. the temperature T , which we shall express in units of T_c , by means of $t = T/T_c$;
3. the plasma frequency Ω_2 and the saturation value τ_2 for the relaxation time of the outer plates;
4. the dielectric constant $\epsilon_1(0)$ of the insulating gaps;
5. the plasma frequency Ω_n and the saturation value τ_n for the relaxation time of the film, in its normal state;
6. the BCS gap $\Delta(T)$ of the superconducting film.

Some simple properties of our expression for $\Delta F_E^{(C)}(T)$ are obvious. First, it is clear from Eq. (13) that $Q_I^{TE/TM}(\zeta, p) \rightarrow 1$ for $L \rightarrow \infty$, and thus $\Delta F_E^{(C)} \rightarrow 0$ in this limit, as it should. Another important limit is that for $L \rightarrow 0$. In this limit, $\Delta F_E^{(C)}$ approaches a *finite* value, because, as pointed earlier, for large ζ the permittivities of the film in the normal and in the superconducting states become undistinguishable, and then the ratios $Q_n^{TE/TM}/Q_s^{TE/TM}$ approach one (and their logarithms approach zero) faster than $Q_{n/s}^{TE/TM}$, and this ensures convergence of Eqs. (12) and (15) also for $L = 0$.

We consider now the dependence of $\Delta F_E^{(C)}(T)$ on D . For $D \rightarrow \infty$, the expressions of $Q_I^{TE/TM}$ reduce to

$$\lim_{D \rightarrow \infty} Q_I^{TE/TM} = (1 - \Delta_{1I}^{TE/TM} \Delta_{12}^{TE/TM} e^{-2\zeta K_1 L/c})^2, \quad (19)$$

which coincides with the square of the analogous expression for a three-layer cavity consisting only of the outer plate, the insulating layer and an infinite superconducting layer. Upon taking the logarithm of $Q_I^{TE/TM}$ we thus obtain that $\Delta F_E^{(C)}$ is twice the value for the three-layer system, which is what one would have expected since in the limit $D \rightarrow \infty$ our five-layered cavity becomes equivalent to a system of two identical three-layered cavities. The rate of approach to the limiting double three-layer system is controlled by the exponential factors $\exp(-2DK_{n/s}\zeta/c)$, which set the scale D_0 above which $\Delta F_E^{(C)}$ becomes independent of D and reaches its $D \rightarrow \infty$ limiting value. The value of D_0 can be estimated as follows. For photon frequencies ζ of order $\bar{\zeta} = 2\Delta/\hbar$, which are the relevant ones for $\Delta F_E^{(C)}$, it turns out that $\epsilon_s(i\zeta) > \epsilon_n(i\zeta)$ (see Appendix B), and therefore we have that $K_s(\zeta, p) > K_n(\zeta, p) > K_n(\zeta, 0)$. On the other hand, using the Drude model Eq. (17) for $\epsilon_n(i\zeta)$ we estimate $\zeta K_n(\zeta, 0) \approx \zeta \sqrt{\epsilon_n(i\zeta)} \approx \Omega_n/\sqrt{1+y}$, which implies

$$\exp(-2DK_{n/s}\zeta/c) < \exp\left(-\frac{2D\Omega_n}{c\sqrt{1+y}}\right).$$

We see from this Equation that the exponential becomes negligible for $D \gg D_0$, where

$$D_0 = \frac{c}{2\Omega_n} \sqrt{1+y}. \quad (20)$$

For a typical value of the plasma frequency $\hbar\Omega_n \simeq (10 \div 20)$ eV, we thus obtain

$$D_0 \approx 10 \text{ nm}.$$

The above number is very important for us, because it provides an estimate of the thickness D of the film, for which the largest shift of critical field should be expected. Indeed, we see from Eq. (7) that the largest shift is obtained for the value of D that maximizes the ratio $\Delta F_E^{(C)}/\mathcal{E}_{\text{cond}}$. Now, the condensation energy $\mathcal{E}_{\text{cond}} = V e(T)$ is proportional to the volume V of the film and then to D (in reality, for certain superconductors and for ultrathin films with $D \ll \lambda, \xi$ the critical temperature T_c and then the density of condensation energy $e(t)$ may depend on D . See discussion on Be films in the next Subsection). Therefore, for $D \gg D_0$, when $\Delta F_E^{(C)}$ becomes independent of D , the ratio $\Delta F_E^{(C)}/\mathcal{E}_{\text{cond}}$ decreases like $1/D$ because of the unlimited increase of $\mathcal{E}_{\text{cond}}$ with D . It then follows that the optimal values of D must be of order D_0 or so, i.e. of a few nm, and this is the range that we shall consider in what follows.

B. Numerical computation of the variation of Casimir free energy

The variation of Casimir free energy $\Delta F_E^{(C)}(T)$, Eq. (15), has been computed numerically. For a superconducting film with a critical temperature T_c , the gap $\Delta(T)$ has been estimated by using the approximate BCS formula Eq. (A13). In what follows we present some of our results in terms of the so-called impurity parameter $y = \hbar/(2\Delta(T)\tau_n)$, which is commonly used, in place of the relaxation time τ_n , as a convenient measure of the degree of purity of the superconductor. In the range of parameters that we consider, the value of $\Delta F_E^{(C)}$ is independent, to better than four significant digits, of the value of $\epsilon_1(0)$, for $1 < \epsilon_1(0) < 300$. In all computations presented below, we fix once and for all $\epsilon_1(0) = 100$.

Another important remark is that, in all cases that we considered, the contribution of TM modes to $\Delta F_E^{(C)}$ is completely negligible, being three or four orders of magnitude smaller than that of TE modes. We postpone to next Section a discussion of the implications of this fact.

In Fig. 2 we show the plot of $\Delta F_E^{(C)}$ (in erg) as a function of the width L (in nm) of the insulating gap, for $D = 5$ nm, $T_c = 0.5$ K, $y = 15$, $t = 0.9$, $\Omega_n = \Omega_2 = 18.9$ eV, $\tau_2 = 2.4 \times 10^{-12}$ sec. We observe that $\Delta F_E^{(C)}$ is always *positive*, which corresponds to the intuitive expectation that transition to superconductivity of the film leads to a *stronger* Casimir effect, i.e. to *lower* Casimir free energy. The data can be fit very accurately by a curve of

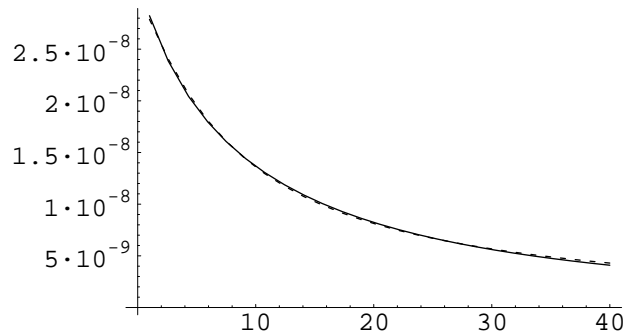


FIG. 2: Plots of $\Delta F_E^{(C)}$ (in erg) as a function of L (in nm) for $D = 5$ nm, $T_c = 0.5$ K, $t = 0.9$. See text for the values of the other parameters. Also shown is the plot (dashed line) of a fit of the type $1/(1 + (L/L_0)^\alpha)$, with $L_0 = 8.3$ nm and $\alpha = 1.15$.

the type

$$\Delta F_E^{(C)}(L) \propto \frac{1}{1 + (L/L_0)^\alpha}, \quad (21)$$

where $L_0 = 8.3$ nm and $\alpha = 1.15$. We thus see, as anticipated earlier, that $\Delta F_E^{(C)}(L)$ approaches a finite limit for $L \rightarrow 0$. This feature of $\Delta F_E^{(C)}$ is helpful, from an experimental point of view, because it implies that the possible roughness of the film and of the lateral plates will have little influence on the value of $\Delta F_E^{(C)}$, for L sufficiently small. By contrast, we recall that the roughness of the surfaces is one of the main sources of uncertainty in the theoretical analysis of standard measurements of the Casimir force, for submicron separations [3].

In Fig. 3 we show the plots of $\Delta F_E^{(C)}$ (in erg), as a function of the impurity parameter y , for the following three combinations of values of the plasma frequencies for the film and the lateral plates: $\Omega_n = \Omega_2 = 18.9$ eV (solid curve), $\Omega_n = 18.9$, $\Omega_2 = 12$ eV (point-dashed curve) and $\Omega_n = \Omega_2 = 12$ eV (dotted curve) (the values of 18.9 eV and 12 eV correspond respectively, to Be and Al). All curves have been computed for $L = 10$ nm, $D = 5$ nm, $T_c = 0.5$ K, $t = 0.9$, $\tau_2 = 2.4 \times 10^{-12}$ sec. We see that $\Delta F_E^{(C)}$ has a maximum for $y \simeq 10 \div 15$. While the decrease of $\Delta F_E^{(C)}$ for large values of y is obvious, it is perhaps surprising to see that it decreases also when y becomes very small, i.e. when the degree of purity of the film is improved. In fact, this latter behavior is explained by observing that, for small values of y , the film is so pure that already in the normal state, it behaves as a very good conductor and then transition to superconductivity cannot increase significantly the Casimir energy. Notice also that $\Delta F_E^{(C)}$ is very sensitive to the values for the plasma frequencies both of the film and of the lateral plates, and it increases sensibly when either one is increased.

In Fig. 4 we show the plot of $\Delta F_E^{(C)}$ as a function of

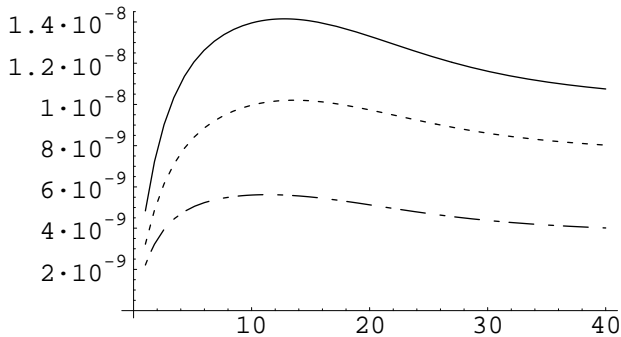


FIG. 3: Plots of $\Delta F_E^{(C)}$ (in erg) for $L = 10$ nm, $D = 5$ nm, $T_c = 0.5$ K and $t = 0.9$, as a function of the impurity parameter y , for $\Omega_n = \Omega_2 = 18.9$ eV (solid line), $\Omega_n = 18.9$, $\Omega_2 = 12$ eV (dashed line) and for $\Omega_n = \Omega_2 = 12$ eV (point-dashed line). See text for values of the other parameters.

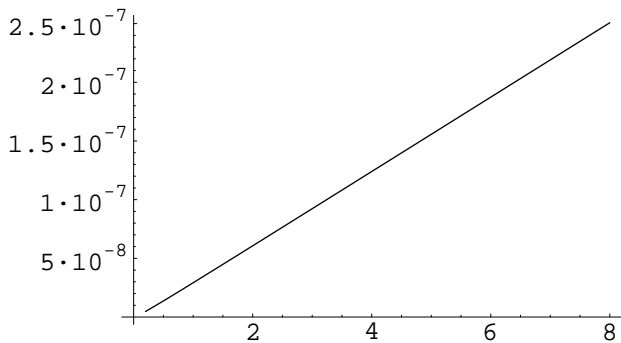


FIG. 4: Plots of $\Delta F_E^{(C)}$ (in erg) as a function of T_c (in K) for $L = 10$ nm, $D = 5$ nm, $y = 15$ and $t = 0.9$. See text for values of the other parameters.

the critical temperature T_c of the film, for $L = 10$ nm, $D = 5$ nm, and $t = 0.9$. All other parameters are as in Fig. 2. The figure shows that $\Delta F_E^{(C)}$ depends linearly on T_c .

In Fig. 5 we show the plot of $\Delta F_E^{(C)}$ as a function of t , for $T_c = 0.5$ and $\tau_n = 5 \times 10^{-13}$ sec (all other parameters are as in Fig. 4). Notice that in this plot we are holding τ_n constant and hence, by virtue of the temperature dependence of the gap $\Delta(T)$ (see Eq. (A13)), the impurity parameter y is not constant (for $T = 0$, we have $y(0) = 8.7$). Note also that, for $T/T_c \rightarrow 1$, $\Delta F_E^{(C)}$ approaches zero linearly in $(1 - t)$. Also shown in the Figure (dashed line) is the plot of the low-temperature approximation to $\Delta F_E^{(C)}$, obtained by replacing the Matsubara sum Eq. (15) by the integral over ζ , as in Eq. (12). This approximation was used in Ref. [8], and as we see from Fig. 5 it works fairly well in the whole range of temperatures. For the explanation of the third curve (point-dashed line) shown in Fig. 5, see next Subsection.

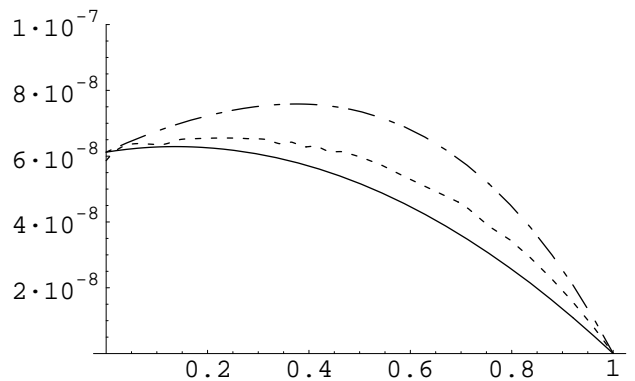


FIG. 5: Plot (solid line) of $\Delta F_E^{(C)}$ (in erg) as a function of t for $L = 10$ nm, $D = 5$ nm, $T_c = 0.5$ K, $\tau_n = 5 \times 10^{-13}$ sec. The point-dashed line includes the contribution of the TE zero mode, computed using the plasma model for the lateral plates. Also shown (dashed line) is the plot of the low-temperature limit of the Matsubara sum, Eq. (12). See text for further details.

C. Contribution from the TE zero mode.

In the current literature on thermal corrections to the Casimir effect there is an ongoing controversy concerning the proper way of calculating the contribution of the TE zero mode (i.e. the $l = 0$ term in the Matsubara sum) to the Casimir free energy (see Refs. [11] for a detailed discussion of different points of view on this problem). The essence of the question is whether one can use the Lifshitz theory to evaluate the TE zero mode, and in the affirmative case, for what choice of the metal permittivity function $\epsilon(i\zeta)$. Indeed, all the trouble arises from the fact that the computation of this mode involves the quantity C :

$$C := \lim_{\zeta \rightarrow 0} (\zeta^2 \epsilon(i\zeta)). \quad (22)$$

If one uses the Drude function Eq. (17) (with a finite value of τ) one obtains $C = 0$, and this implies that the TE zero mode gives zero contribution to the Casimir free energy, irrespective of how large τ is. On the contrary, if one uses the simpler plasma model that gives

$$\epsilon(i\zeta) = 1 + \frac{\Omega_p^2}{\zeta^2} \quad (23)$$

one finds $C = \Omega_p^2$, and then the zero mode gives a non vanishing contribution, reproducing the ideal metal case in the limit of infinite plasma frequency. While we address the reader to Refs. [11] for a discussion of the reasons in favor of the alternative approaches to this question that have been proposed by a number of authors, we would like to examine the consequences of this problem for our computation of $\Delta F_E^{(C)}$.

All computations presented in the previous Section used the Drude model for the permittivities for both the

lateral plates and the film, in the normal state. Since, as pointed out earlier, the contribution from the TM modes is negligible, it follows that the values of $\Delta F_E^{(C)}$ that we computed receive no contribution from the TE zero mode.

It is interesting to see what happens in our computations if, in the evaluation of the zero mode, we replace the Drude model by the plasma model. We shall do it only for the lateral plates. For the superconducting film we prefer keep using the Drude model, since it is the one to which the BCS formula of the permittivity converges for $T \rightarrow T_c$. Thus, if we denote by $\Delta F_E^{(C)}(TE \text{ z.m.})$ the contribution of the TE zero mode, we obtain for the total variation of Casimir free energy the expression

$$\widetilde{\Delta F}_E^{(C)} = \Delta F_E^{(C)}(TE \text{ z.m.}) + \Delta F_E^{(C)}. \quad (24)$$

In Fig. 5 we plot (dashed line) $\widetilde{\Delta F}_E^{(C)}$ as a function of t , while in Fig. 6 we show the ratio $\Delta F_E^{(C)}(TE \text{ z.m.})/\Delta F_E^{(C)}$, again as a function of t (all parameters are as in Fig. 5). We observe that the weight of the zero mode increases as we approach T_c . The reason of this is easy to understand: the zero mode becomes more and more important because a decreasing number of Matsubara modes contribute to $\Delta F_E^{(C)}$, as one approaches T_c . This is so because the quantities $(Q_n^{TE}/Q_s^{TE})(i\zeta)$ that occur in Eq. (15) are substantially different from one only for complex frequencies ζ of order of a few tens of times kT_c/\hbar . Since the l -th Matsubara mode has a frequency equal to $2\pi l kT/\hbar$, it is clear that the number of terms effectively contributing to $\Delta F_E^{(C)}$ should be roughly proportional to T_c/T , and hence it is large for $T \ll T_c$, but becomes small for T comparable to T_c . Notice that close to T_c the contribution of the zero mode is practically of the same magnitude as that of $\Delta F_E^{(C)}$ and therefore its inclusion doubles the variation of Casimir free energy.

D. Shift of critical field

Having estimated the variation of Casimir energy $\Delta F_E^{(C)}$ across the transition, we are now ready to compute the shift of parallel critical field, using Eq. (5). The result depends of course on the superconductor, and in order to get a feeling of what to expect depending on this choice, it is convenient to consider the approximate expression for the relative shift Eq. (7). According to this formula, the shift is larger when $\mathcal{E}_{\text{cond}}$ is smaller and/or $\Delta F_E^{(C)}$ is larger. Now, we see from Fig. 4 that $\Delta F_E^{(C)}$ is almost proportional to T_c , while from Eqs. (A4) and (A5) in Appendix A we see $\mathcal{E}_{\text{cond}}(T) \propto H_c^2(0)$. Therefore, if we forget for a moment other influential factors (like the values for the impurity parameter y , the plasma frequency and the relaxation time that we shall consider

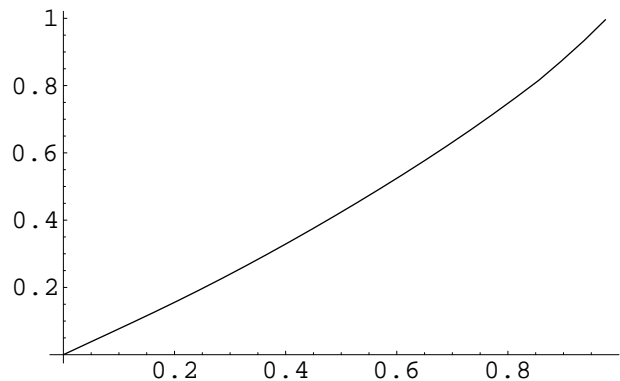


FIG. 6: Plot of the ratio $\Delta F_E^{(C)}(TE \text{ z.m.})/\Delta F_E^{(C)}$ as a function of t . All parameters are same as in Fig. 5. $\Delta F_E^{(C)}(TE \text{ z.m.})$ is evaluated using the plasma model for the outer plates.

TABLE I: Values of T_c (in K), $H_c(0)$ (in Oe) and $s = H_c^2(0)/T_c$ in (Oe²/K) for some type I superconductors.

	T_c	$H_c(0)$	$H_c^2(0)/T_c$
Be	0.024	1.08	48.5
Zn	0.88	53	3192
Al	1.2	105	9343
Sn	3.72	306	25171

later) we obtain from Eq. (7) the estimate

$$\frac{\delta H_{c\parallel}}{H_{c\parallel}} \approx \frac{\Delta F_E^{(C)}}{2\mathcal{E}_{\text{cond}}(T)} \propto \frac{T_c}{H_c^2(0)}. \quad (25)$$

We thus see that the relative shift should be inversely proportional to the quantity $s := H_c^2(0)/T_c$, and so superconductors with small values of s should be preferable. Now, if we use the empirical law Eq. (A6) to estimate the dependence of $H_c(0)$ on the critical temperature of the superconductor, we find that s goes like $T_c^{1.6}$, and this implies that we should first consider superconductors with low T_c . In reality, things are not so simple. Consider for example the case of Be. It has a very low $T_c = 24$ mK, and a correspondingly low $H_c(0) = 1.079 \pm 0.002$ Oe [28], giving $s = 48.5$ Oe²/K, which is much smaller than the values of s for other superconductors. As a comparison, we quote in Table I the values of T_c , $H_c(0)$ and s for a number of type I superconductors. From these data it would seem that Be should give a great advantage over other superconductors. However, unfortunately, the above low value of T_c refers to bulk samples, while very thin Be films (with thicknesses of a few nm) have a much higher T_c . For example, the authors of Ref. [27] report a T_c of 0.5 K for a thickness of 5 nm. The value of the condensation energy for such a film is not reported in Ref. [27], but one can estimate that $\mathcal{E}_{\text{cond}}$ scales with respect to the bulk value in the same proportion as the square of the critical temperature (see Appendix A). If we insist

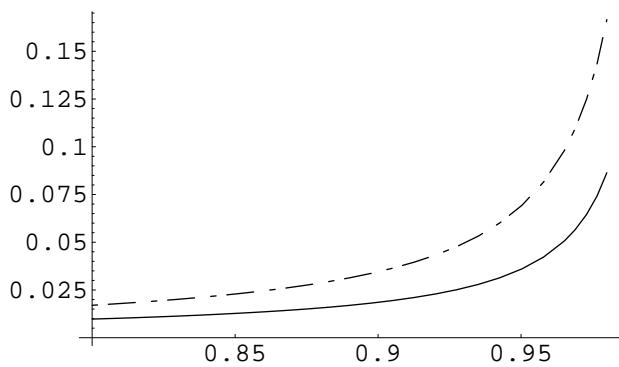


FIG. 7: Plot (solid line) of the relative shift of parallel critical field for a Be cavity, as a function of T/T_c . The point-dashed line includes the contribution of the TE zero modes, evaluated as in Fig. 5. All parameters are as in Fig. 5.

in expressing the condensation energy in the form of Eq. (A5), this amounts to saying that the thermodynamical field of a thin film scales with its critical temperature. This gives us an estimate of $H_c(0) = 22.5$ Oe for the films of Ref. [27], and thus we find $s = 1010$ Oe²/K, which is much worse than the bulk value, but still good compared with other type I superconductors.

We consider now the other factors affecting the relative shift of critical field, that we have neglected in the above discussion. The first important factor is the value of the plasma frequency Ω . As we see from Fig. 3, larger values of Ω both for the film and the lateral plates lead to significantly larger values for $\Delta F_E^{(C)}$. Now we recall that Be has $\hbar\Omega = 18.9$ eV, which is much larger than the value for other metals (for example Al, which has $\hbar\Omega = 12$ eV). Therefore it would be advantageous to use this material both for the film and the lateral plates. In this respect, the circumstance that the critical temperature of a thin Be film is much higher than the bulk value can be exploited to our advantage, as it allows to use Be both for the film and the lateral thick plates, leaving us with a wide range of temperatures for which the film is superconducting, while the lateral mirrors are normal, as we require. According to Fig. 3, we can gain in this way a factor larger than two, with respect to say, a cavity made solely of Al. Another reason in favor of Be is related to the fact that the critical field $H_{c\parallel}$ of thin films is not defined in general as sharply as in bulk samples, and one rather has a fuzzy critical region of finite width. It is clear therefore that preference should be given to materials for which this indeterminacy is smallest. It turns out that Be can be deposited in ultrathin films, characterized by an extraordinary degree of uniformity. A consequence of this uniformity is that even for thicknesses D of a few nm, Be films possess very sharp parallel critical magnetic fields $H_{c\parallel}$, that can be measured with a precision of a few parts in a thousand [27].

Having collected a number of arguments in favor of Be, we can now show the results of our computations

for the shift of critical field. In Fig. 8 we show (solid line) the relative shift of the critical parallel field of a Be film, as a function of t . Note that, according to Eq. (7) this quantity is independent of the coefficient ρ , whose precise value is in general not known accurately. The Figure has been drawn using the same parameters as in Fig. 5. We show also (point-dashed curve) the relative shift that is obtained after including the contribution of TE zero modes, computed in the way explained in the previous Subsection. We see that this inclusion produces almost a doubling of the shift.

Note that the shift is *positive*, meaning that the critical field for the film placed in the cavity is *larger* than the critical field for an identical film outside the cavity. The increase of critical field relative shift as one approaches the critical temperature arises because, for $t \rightarrow 1$, $\Delta F_E^{(C)}$ and $\mathcal{E}_{\text{cond}}$ approach zero at different rates. Indeed, while $\mathcal{E}_{\text{cond}}$ vanishes as $(1-t)^2$ (see Eq. (A4)), we see from Fig. 5 that $\Delta F_E^{(C)}$ vanishes essentially like the first power of $1-t$.

V. CONCLUSIONS AND DISCUSSION

We have studied a superconducting Casimir cavity, including a thin superconducting film and we have shown that the variation of Casimir free energy, accompanying the superconducting transition, determines a measurable shift of the critical magnetic field required to destroy the film superconductivity. This constitutes a novel approach to the study of the Casimir effect, in which the central role is played by the Casimir energy itself, rather than the Casimir force, as in all experiments performed so far.

Our scheme, apart from its novelty, presents a number of appealing features. The first advantage stems from the fact that it uses *rigid* cavities. As is well known, the experimental difficulty of controlling the parallelism among macroscopic plane plates with submicron separations led the experimenters to consider simpler geometries that do not suffer from this problem, like the sphere-plane one, which has been adopted in all precision experiments on the Casimir force (with the only exception of the experiment by Bressi et al. [1], where the plane-parallel configuration is used). This limitation has made it impossible so far to explore experimentally one of the most intriguing features of the Casimir effect, i.e. its dependence on the geometry of the cavity. The use of rigid cavities, as in our approach, might make it easier to realize a number of geometries that are difficult to realize within the standard force-measurements scheme.

Another interesting feature of our scheme, not mentioned in Ref. [8], is its sensitivity to the contribution from the TE zero mode. This is a controversial issue in the current literature on thermal corrections to the Casimir effect. It is well known that, for submicron plate separations, thermal corrections are negligible at cryogenic temperature, and become relevant only at room temperature. However, this is not the case in our su-

perconducting cavities, because the shift of critical field is completely determined by the Matsubara modes with frequencies below or of order kT_c/\hbar , which is where the reflective properties of a film change when it becomes superconducting. As a consequence, as we have shown in Sec. IV C, different treatments of the TE zero mode lead to strongly different predictions for the shift of critical field, at the level of doubling the shift close to T_c , and this opens the way to a possible experimental clarification of this delicate problem.

Our computations show that larger shifts of the critical field can be obtained by employing for the lateral plates and the superconducting film materials with high plasma frequencies, which ensure a high reflection coefficient. We found also that it is advantageous to use films with a value of the impurity parameter y about $10 \div 15$. Such values of y require films with rather large free mean paths, of order 100 nm or so, which can be difficult to reach in ultrathin films with thicknesses of $5 \div 10$ nm, as we require. Finally, since larger relative shifts are found near the critical temperature, an effort should be made to produce ultrathin films with high degree of purity, in order to obtain narrow transition regions, with sharply defined critical temperatures.

It is also the case to note that the variation of Casimir free energy $\Delta F_E^{(C)}$ approaches a finite limit, for vanishing separation L of the film from the outer plates. For separations of order 10 nm, this behavior of $\Delta F_E^{(C)}$ ensures a good degree of robustness of the resulting shift of critical field with respect to the roughness of the metal surfaces, which is known to give an important contribution in standard Casimir force measurements, for submicron separations [3]. Equally helpful in this respect is the fact that $\Delta F_E^{(C)}$ is independent, to a high accuracy level, of the dielectric function of the insulating layers separating the film from the outer plates.

It would be very interesting to obtain an experimental verification of the phenomena described in this paper. Indeed this is the aim of the ALADIN experiment, sponsored by INFN, which is currently under way at the Dipartimento di Scienze Fisiche dell'Università di Napoli Federico II. Some details about the experimental setup are now helpful. In order to detect the shift in the critical field of a thin superconducting film resulting from the Casimir effect, we foresee to simultaneously deposit on a single substrate a certain number of superconducting films of same thickness, covered with a thin insulating layer, again of same thickness for all films. Half of these films will then be covered with a third thick layer of a non-superconducting metal, thus forming a three-layer Casimir cavity. Such three-layer systems are easier to manufacture than the five-layer cavities discussed in this paper, and thus, even if they lead to a smaller effect, will be considered first. Passage to the five-layer case is expected at a later stage, and will be dealt with in a similar way. The simultaneous deposition as above is aimed at ensuring that all superconducting films, both the single ones and those in the cavities, have the same properties

(thickness, degree of purity etc.). We plan to repeat the measurements for various film and oxide thicknesses, in order to test our theoretical predictions.

Besides the authors of the present paper, the experiment ALADIN has involved D. Born, A. Cassinese, F. Chiarella, L. Milano, O. Scaldaferrri, F. Tafuri, and R. Vaglio.

Acknowledgments

We would like to thank A. Cassinese, F. Tafuri, A. Tagliacozzo and R. Vaglio for valuable discussions, G.L. Klimchitskaya and V.M. Mostepanenko for enlightening discussions on several aspects of the problem. G.B. and G.E. acknowledge partial financial support by PRIN *SIN-TESE*.

VI. APPENDICES

For the convenience of the reader, we briefly review in these Appendices the basic properties of type I superconductors, that are important for the superconducting Casimir cavities to be considered later. For a more complete discussion, we address the reader to the monograph [24].

APPENDIX A: MAGNETIC PROPERTIES OF TYPE I SUPERCONDUCTORS

As is well known, superconductors tend to expel magnetic fields from their interior (*Meissner effect*). The reversibility of this effect implies the existence of a well defined critical magnetic field H_c that destroys superconductivity, via a first-order phase transition. If we denote by $e(T)$ the difference between the zero-field Helmholtz free energies (per unit volume) $f_n(T)$ and $f_s(T)$ in the normal (n) and the superconducting (s) states respectively, i.e.

$$e(T) := f_n(T) - f_s(T), \quad (\text{A1})$$

($e(T)$ is called the condensation energy of the superconductor) it can be shown that the value of H_c is related to $e(T)$ by the relation

$$\frac{H_c^2(T)}{8\pi} = e(T). \quad (\text{A2})$$

Upon using the well known empirical parabolic law for H_c :

$$H_c(T) \approx H_c(0) (1 - t^2), \quad (\text{A3})$$

where $t = T/T_c$ with T_c the critical temperature, it follows from Eq. (A2) that the condensation energy has the following dependence on t :

$$e(T) = e(0) (1 - t^2)^2, \quad (\text{A4})$$

where

$$e(0) = \frac{H_c^2(0)}{8\pi}. \quad (\text{A5})$$

Another empirical law of interest [25] is the one giving the approximate dependence of $H_c(0)$ on T_c (valid for type I superconductors)

$$H_c(0) \propto T_c^{1.3}, \quad (\text{A6})$$

and then by using Eq. (A5) we obtain an estimate of the dependence of $e(0)$ on the critical temperature of the superconductor in the form

$$e(0) \propto T_c^{2.6}. \quad (\text{A7})$$

In the case of a thin film, of thickness $D \ll \lambda, \xi$ (with λ the penetration depth and ξ the correlation length), placed in a parallel magnetic field, expulsion of the magnetic field is incomplete, and consequently the critical field increases from H_c to $H_{c\parallel}$. Unlike the bulk case, the transition to the normal phase is of second order, since sufficiently thin films and use of the Ginzburg–Landau theory show that $H_{c\parallel}$ is proportional to $H_c(T)$

$$H_{c\parallel}(T) = \rho(T) H_c(T). \quad (\text{A8})$$

The coefficient ρ has the approximate expression

$$\rho \approx \sqrt{24} \frac{\lambda}{D} \left(1 + \frac{9D^2}{\pi^6 \xi^2} \right), \quad (\text{A9})$$

where the second term inside the brackets accounts for surface nucleation. Upon using Eq. (A8) to express $H_{c\parallel}$ in terms of H_c , we can recast Eq. (A2) in the form

$$\frac{1}{8\pi} \left(\frac{H_{c\parallel}(T)}{\rho} \right)^2 = e(T). \quad (\text{A10})$$

Recalling that the temperature dependence of λ can be approximately described by the law

$$\lambda(T) \approx \lambda(0) [1 - (T/T_c)^4]^{-1/2}, \quad (\text{A11})$$

it follows from Eq. (A10) that, close to T_c , $H_{c\parallel}$ approaches zero like $\sqrt{1 - T/T_c}$.

In the case of ultrathin films (with thicknesses of a few nm) the magnetic behavior can be quite different because the orbital currents are suppressed, and the transition to the normal state is driven by coupling of the magnetic field to the electronic spins. Under such circumstances, the critical field transition can be strongly hysteretic, below a tricritical point [26]. However, close to T_c , there is no hysteresis, and if the films are very pure it is still possible to observe very sharp transitions, with well defined critical fields (defined to within a few parts in a thousand) [27].

It is important to point out that the critical temperature T_c of a thin film does not coincide in general with the bulk value, and it depends on the film thickness and

on the preparation procedure. For example, in the case of thin Beryllium films one can have a T_c as high as 9 K, to be contrasted with the bulk value of 24 mK [30]. In such cases, the condensation energy of the film should not be expected to be the same as for the bulk material. However, one can estimate it by using the BCS formula for the condensation energy (per unit volume) at absolute zero:

$$e(0) = \frac{1}{2} N(0) \Delta^2(0), \quad (\text{A12})$$

where $N(0)$ is the density of electronic states of one spin in the normal metal at the Fermi surface [31]. If we assume that the gap $\Delta(T)$ is always given by the approximate BCS formula [34]

$$2\Delta(T) = 3.528 k T_c \sqrt{1 - \frac{T}{T_c}} \left(0.9963 + 0.7735 \frac{T}{T_c} \right), \quad (\text{A13})$$

and that $N(0)$ for the film is not much different from the bulk value, we obtain from Eq. (A12)

$$\frac{e(0)|_{\text{film}}}{e(0)|_{\text{bulk}}} = \frac{T_c^2|_{\text{film}}}{T_c^2|_{\text{bulk}}}. \quad (\text{A14})$$

If we further assume that the temperature dependence of the condensation energy of a film is still of the form Eq. (A4), the same ratio is found also for the free energies at finite values of t .

APPENDIX B: HIGH-FREQUENCY ELECTRODYNAMICS

As is well known, superconductors show finite dissipation when traversed by alternating currents and/or time-varying electromagnetic fields. At frequencies ω much smaller than the energy gap, $\hbar\omega \ll \Delta(T)$, a qualitative description of the superconductor response is provided by the simple Casimir–Gorter two-fluid model, which leads to the following expression for the real part $\sigma'(\omega)$ of the complex conductivity $\sigma(\omega)$:

$$\sigma'(\omega) = (\pi n_s e^2 / 2m) \delta(\omega) + (n_n e^2 \tau_n / m) (1 + \omega^2 \tau_n^2)^{-1}, \quad (\text{B1})$$

where $\delta(\omega)$ is the Dirac delta function, m and e denote the electron mass and charge, n_s and n_n are the temperature dependent densities of the superconducting and normal electron respectively, and τ_n is the residual relaxation time for the normal electrons, as determined by the impurities present in the sample. As we see, the normal fluid contribution implies a *nonzero* dissipation at *all nonzero frequencies*. The delta function contribution, proportional to n_s is a dc contribution, ensuring fulfillment of the oscillator strength sum rule:

$$\int_0^\infty d\omega \sigma'(\omega) = \frac{\pi n e^2}{2m}, \quad (\text{B2})$$

where $n = n_s + n_n$ is the total electron density.

An accurate description of the complex conductivity of a BCS superconductor, for photon energies up to and larger than (twice) the gap, requires that one uses the full Mattis–Bardeen theory of electric conduction, which is valid also in the domain of the anomalous skin effect [32]. Taking full account of space dispersion, this theory gives rise to an expression of the complex conductivity $\sigma_s(\omega, \mathbf{q})$ that depends also on the spatial wave vector \mathbf{q} . In the case of a BCS conductor at a temperature $T < T_c$, and in the local limit $\mathbf{q} \rightarrow 0$, the resulting expression of $\sigma'_s(\omega)$ can be written in a form analogous to Eq. (B1):

$$\sigma'_s(\omega) = \kappa \delta(\omega) + \hat{\sigma}'_s(\omega). \quad (\text{B3})$$

For $\omega > 0$, $\hat{\sigma}'_s(\omega)$ reads as [33]

$$\hat{\sigma}'_s(\omega) = \frac{\hbar n e^2}{2m\omega\tau_n} \left[\int_{\Delta}^{\infty} dE J_T + \theta(\hbar\omega - 2\Delta) \int_{\Delta - \hbar\omega}^{-\Delta} dE J_D \right], \quad (\text{B4})$$

where

$$J_T := g(\omega, \tau_n, E) \left[\tanh \frac{E + \hbar\omega}{2kT} - \tanh \frac{E}{2kT} \right] \quad (\text{B5})$$

$$J_D := -g(\omega, \tau_n, E) \tanh \left(\frac{E}{2kT} \right), \quad (\text{B6})$$

with k the Boltzmann constant. Defining

$$P_1 := \sqrt{(E + \hbar\omega)^2 - \Delta^2}, \quad P_2 := \sqrt{E^2 - \Delta^2}, \quad (\text{B7})$$

the function $g(\omega, \tau_n, E)$ is

$$g := \left[1 + \frac{E(E + \hbar\omega) + \Delta^2}{P_1 P_2} \right] \frac{1}{(P_1 - P_2)^2 + (\hbar/\tau_n)^2} - \left[1 - \frac{E(E + \hbar\omega) + \Delta^2}{P_1 P_2} \right] \frac{1}{(P_1 - P_2)^2 + (\hbar/\tau_n)^2}.$$

The coefficient κ of the delta function in Eq. (B3) is again determined so as to satisfy the sum rule Eq. (B2) and can be computed exactly according to [33]

$$\kappa = \frac{\pi n e^2}{m} \left[\frac{\pi \tau_n \Delta}{\hbar} \tanh \frac{\Delta}{2kT} - 4\Delta^2 \int_{\Delta}^{\infty} dE \frac{\tanh(E/2kT)}{\sqrt{E^2 - \Delta^2} [4(E^2 - \Delta^2) + (\hbar/\tau_n)^2]} \right]. \quad (\text{B8})$$

The conductivity $\sigma'_s(\omega)$ in Eq. (B3) can be thought of as the sum of three contributions: a δ function at the origin, a broad thermal component that diverges logarithmically at $\omega = 0$ and a direct absorption component, with an onset at $2\Delta(T)$ (see the second in Ref. [33]). At any $T < T_c$, complete specification of $\sigma'_s(\omega)$ requires three parameters: besides the free electron density n (or equivalently the square of the plasma frequency $\Omega_n^2 = 4\pi n e^2/m$) that provides the overall scale of σ'_s , and the relaxation time for the normal electrons τ_n , both of which already occur in the simple Drude formula Eq. (B9) below, $\sigma'_s(\omega)$ only depends on one extra parameter, i.e. the gap Δ . In fact, after the frequencies are expressed in reduced units $x = \hbar\omega/(2\Delta)$, the expression inside the brackets on the r.h.s. of Eq. (B4) becomes a function solely of x , $2\Delta/(kT)$ and the so-called impurity parameter $y = \hbar/(2\Delta\tau_n)$. We point out that this expression for σ'_s is valid for arbitrary relaxation times τ_n , i.e. for arbitrary mean free paths, and in particular it holds in the so-called impure limit $y = 2\Delta/(\hbar\tau_n) \gg 1$, where the effects of non-locality become negligible. We recall that the gap Δ is a temperature dependent quantity. In our numerical computations, we used for it the approximate formula Eq. (A13).

We point out that at fixed ω for $T \rightarrow T_c$, as well as at fixed $T < T_c$ for $x \rightarrow \infty$, $\sigma'_s(\omega)$ approaches the Drude

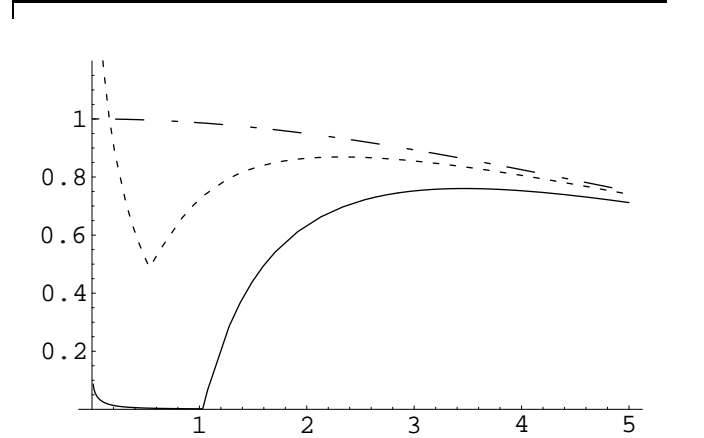


FIG. 8: Plots of $m\sigma'_s(\omega)/(ne^2\tau_n)$, for $T/T_c = 0.3$ (solid line), $T/T_c = 0.9$ (dashed line) and $T = T_c$ (point-dashed line). On the abscissa, the frequency ω is in reduced units $x_0 = \hbar\omega/(2\Delta(0))$, and $y_0 = 2\Delta(0)/\tau_n \simeq 8.7$.

expression $\sigma'_D(\omega)$

$$\sigma'_D(\omega) = \frac{1}{4\pi} \frac{\Omega^2 \tau}{1 + \omega^2 \tau^2}. \quad (\text{B9})$$

The convergence of $\sigma'_s(\omega)$ to $\sigma'_D(\omega)$ in the frequency domain is in fact very fast, and already for x of order 10 or so σ'_s becomes undistinguishable from σ'_D , in ac-

cordance with experimental findings [13]. In Fig. 5, we show the plots of $\sigma'_s(\omega)m/(ne^2\tau_n)$, for $T/T_c = 0.3$, $T/T_c = 0.9$ and $T = T_c$. The curves are computed for $y_0 = 2\Delta(0)/\tau_n \simeq 8.7$. Frequencies are measured in reduced units $x_0 = \hbar\omega/(2\Delta(0))$.

As we see from Eqs. (12) and (15) the expression for the variation of Casimir free energy involves the permittivity of the superconducting film $\epsilon_s(i\zeta)$ for complex frequencies $i\zeta$. Now, $\epsilon_s(i\zeta)$ cannot be given in closed form, and we have estimated it as follows. First, by using well known dispersion relations, we express $\epsilon_s(i\zeta)$ in terms of the imaginary part $\epsilon''_s(\omega)$ of the dielectric permittivity $\epsilon_s(\omega) = \epsilon'_s(\omega) + i\epsilon''_s(\omega)$ at real frequencies, i.e.

$$\epsilon_s(i\zeta) - 1 = \frac{2}{\pi} \int_0^\infty d\omega \frac{\omega \epsilon''_s(\omega)}{\zeta^2 + \omega^2}. \quad (\text{B10})$$

Upon using now the standard relation connecting the imaginariy part of the electric permittivity to the real part of the complex conductivity σ of a metal:

$$\epsilon''(\omega) = \frac{4\pi}{\omega} \sigma'(\omega), \quad (\text{B11})$$

we can rewrite the r.h.s. of Eq. (B10) as

$$\epsilon_s(i\zeta) = 1 + 8 \int_0^\infty d\omega \frac{\sigma'_s(\omega)}{\zeta^2 + \omega^2}. \quad (\text{B12})$$

We now take for $\sigma'_s(\omega)$ the semianalytical BCS formula given in Eqs. (B3-B8). Upon plugging Eq. (B3) into Eq. (B12) we then obtain the following formula for $\epsilon_s(i\zeta)$:

$$\epsilon_s(i\zeta) = 1 + 8 \int_0^\infty d\omega \frac{\hat{\sigma}'_s(\omega)}{\zeta^2 + \omega^2} + \frac{4\kappa}{\zeta^2}, \quad (\text{B13})$$

where κ is given in Eq. (B8). For the purpose of a numerical evaluation of Eq. (B13), it is however convenient to rewrite it in a different form. We recall that the coefficient κ is defined so as to satisfy the sum rule Eq. (B2). Now, upon substituting the expression for $\sigma'_s(\omega)$ Eq. (B3) into Eq. (B2) we obtain

$$\frac{\kappa}{2} + \int_0^\infty d\omega \hat{\sigma}'_s(\omega) = \frac{\pi ne^2}{2m}. \quad (\text{B14})$$

However, the sum rule holds also in the normal state of the film, and thus we have

$$\int_0^\infty d\omega \sigma'_D(\omega) = \frac{\pi ne^2}{2m}, \quad (\text{B15})$$

where $\sigma'_D(\omega)$ (see Eq. (B9)) is the expression derived from Eq. (16), by using Eq. (B11). Upon equating the l.h.s. of the above two Equations, we arrive at the following expression for $\kappa/2$:

$$\frac{\kappa}{2} = \int_0^\infty d\omega (\sigma'_D(\omega) - \hat{\sigma}'_s(\omega)). \quad (\text{B16})$$

Upon plugging this expression for κ into Eq. (B13), and by using the dispersion relation for σ'_D , i.e.

$$\epsilon_D(i\zeta) - 1 = 8 \int_0^\infty d\omega \frac{\sigma'_D(\omega)}{\zeta^2 + \omega^2}, \quad (\text{B17})$$

it is easy to obtain the final equation

$$\epsilon_s(i\zeta) = \epsilon_D(i\zeta) - \frac{8}{\zeta^2} \int_0^\infty d\omega \frac{\omega^2 (\hat{\sigma}'_s(\omega) - \sigma'_D(\omega))}{\zeta^2 + \omega^2}, \quad (\text{B18})$$

that we have used in our numerical computations. It has the virtue of expressing the variation in the film permittivity $\epsilon_s(i\zeta) - \epsilon_D(i\zeta)$ across the transition, as an integral involving the variation of conductivity $\hat{\sigma}'_s(\omega) - \sigma'_D(\omega)$. Indeed, $\hat{\sigma}'_s(\omega) - \sigma'_D(\omega)$ is appreciably different from zero only for frequencies ω of order of a few times kT_c/\hbar , and goes to zero like $1/\omega^3$ for large ω 's, and this ensures rapid convergence of the integral on the r.h.s. of Eq. (B18). By looking at the plots in Fig. (8), we see that, for frequencies of order $2\Delta/\hbar$ (apart from a very narrow region near the origin, where $\hat{\sigma}_s(\omega)$ has a logarithmic behavior), $\hat{\sigma}_s(\omega) < \hat{\sigma}_n(\omega)$, and therefore it follows from Eq. (B18) that $\epsilon_s(i\zeta) > \epsilon_n(i\zeta)$. This relation is fully confirmed by our numerical computations.

-
- [1] S.K. Lamoreaux, Phys. Rev. Lett. **78**, 5 (1997); U. Mohideen and A. Roy, *ibid.* **81**, 4549 (1998); G. Bressi, G. Carugno, R. Onofrio and G. Ruoso, *ibid.* **88**, 041804 (2002); R.S. Decca, D. López, E. Fischbach, and D.E. Krause, *ibid.* **91**, 050402 (2003); H.B. Chan, V.A. Aksyuk, R.N. Kleiman, D.J. Bishop and F. Capasso, Science **291**, 1941 (2001).
- [2] H.B.G. Casimir, Proc. K. Ned. Akad. Wet. Rev. **51**, 793 (1948).
- [3] M. Bordag, U. Mohideen and V.M. Mostepanenko, Phys. Rep. **353**, 1 (2001).
- [4] K. Milton, J. Phys. **A 37**, R209 (2004).
- [5] V.V. Nesterenko, G. Lambiase, and G. Scarpetta, Riv. Nuovo Cim. **27** Ser. 4 No. 6, 1 (2004).
- [6] S. K. Lamoreaux, Rep. Prog. Phys. **68**, 201 (2005).
- [7] S. Weinberg, Rev. Mod. Phys. **61**, 1 (1989); M. Ishak, astro-ph/0504416.
- [8] G. Bimonte, E. Calloni, G. Esposito, L. Milano and L. Rosa, Phys. Rev. Lett. **94**, 180402 (2005).
- [9] T.H. Boyer, Phys. Rev. **174**, 1764 (1968).
- [10] G. Barton, J. Phys. A: Math. Gen. **34**, 4083 (2001).
- [11] B. Geyer, G.L. Klimchitskaya and V. M. Mostepanenko, Phys. Rev. **A 67**, 062102 (2003); J.S. Høye, I. Brevik, J.B. Aarseth and K.A. Milton, Phys. Rev. **E 67**, 056116

- (2003); R.S. Decca, D. Lopez, E. Fischbach, G.L. Klimchitskaya, D.E. Krause, V.M. Mostepanenko, *Ann. Phys. (N.Y.)* **318**, 307 (2005) and references therein.
- [12] E.M. Lifshitz, *Sov. Phys. JETP* **2**, 73 (1956); E.M. Lifshitz and L.P. Pitaevskii, *Landau and Lifshitz Course of Theoretical Physics: Statistical Physics Part II* (Butterworth-Heinemann, 1980)
- [13] R.E. Glover III and M. Tinkham, *Phys. Rev.* **108**, 243 (1957).
- [14] M. Kreuzer and K. Svozil, *Phys. Rev.* **D 34**, 1429 (1985).
- [15] D. Iannuzzi, M. Lisanti and F. Capasso, *Proc. Nat. Ac. Sci. USA* **101**, 4019 (2004).
- [16] M. Boström and Bo E. Sernelius, *Phys. Rev.* **B 61**, 2204 (2000); *ibid.* **B 62**, 7523 (2000) and references therein.
- [17] Yu.S. Barash and V.L. Ginzburg, *Sov. Phys.–Usp. (USA)* **18**, 305 (1975).
- [18] R. Blossey, *Europhys. Lett.* **54**, 522 (2001).
- [19] V.B. Svetovoy and M.V. Lokhanin, *Phys. Rev.* **A 67**, 022113 (2003); R. Esquivel-Sirvent and V.B. Svetovoy, *Phys. Rev.* **A 69**, 062102 (2004); *Phys. Rev.* **B 72**, 045443 (2005).
- [20] Bo E. Sernelius, *Phys. Rev.* **B 71**, 235114 (2005).
- [21] N.G. van Kampen, B.R.A. Nijboer and K. Schram, *Phys. Lett.* **A 26**, 307 (1968); K. Schram, *Phys. Lett.* **A 43**, 283 (1973).
- [22] F. Zhou and L. Spruch, *Phys. Rev.* **A 52**, 295 (1995).
- [23] A. Lambrecht, M.T. Jaekel and S. Reynaud, *Phys. Lett.* **A 225**, 188 (1997); A. Lambrecht and S. Reynaud, *Eur. Phys. J* **D 8**, 309 (2000); G.L. Klimchitskaya, U. Mohideen, V.M. Mostepanenko, *Phys. Rev.* **A 61**, 062107 (2000).
- [24] M. Tinkham, *Introduction to Superconductivity* (McGraw-Hill, Singapore, 1996)
- [25] H.W. Lewis, *Phys. Rev.* **101**, 939 (1956).
- [26] Wehnao Wu and P.W. Adams, *Phys. Rev. Lett.* **73**, 1412 (1995).
- [27] P.W. Adams, P. Herron and E.I. Meletis, *Phys. Rev.* **B 58**, R2952 (1998).
- [28] R.J. Soulen, Jr., J.H. Colwell and W.E. Fogle, *J. Low Temp. Phys.* **124**, 515 (2001).
- [29] P.W. Adams, *Phys. Rev. Lett.* **92**, 067003 (2004).
- [30] K. Takei, K. Makamura and Y. Maeda, *J. Appl. Phys.* **57**, 5093 (1985) and references therein.
- [31] *Superconductivity*, edited by R.D. Parks (Marcel Dekker, New York, 1969)
- [32] D.C. Mattis and J. Bardeen, *Phys. Rev.* **111**, 412 (1958).
- [33] W. Zimmermann, E.H. Brandt, M. Bauer, E. Seider and L. Genzel, *Physica C* **183**, 99 (1991); see also A.J. Berlinsky, C. Kallin, G. Rose and A.C. Shi, *Phys. Rev.* **B 48**, 4074 (1993).
- [34] D.C. Carless, H.E. Hall and J.R. Hook, *J. Low Temp. Phys.* **50**, 605 (1983).
- [35] When comparing the formulae of this paper with those of [3], please note that our L and D correspond, respectively, to d and a of [3], while the TM and TE modes are labelled there by the suffices (1) and (2), respectively. Note also that in our configuration the central layer is constituted by the superconducting film, and not by the vacuum, and then its permittivity, denoted by ϵ_0 in [3], is not equal to 1, but rather to $\epsilon_{n/s}$ depending on the state of the film.